# A Machine Learning Approach for Understanding Power Distribution System Congestion

Emin Ucer*, Mithat Kisacikoglu*, Ali Gurbuz†, Shahinur Rahman* and Murat Yuksel‡
*Dept. of Electrical and Computer Engineering, The University of Alabama, Tuscaloosa, AL
†Dept. of Electrical and Computer Engineering, Mississippi State University, Starkville, MS
‡Dept. of Electrical and Computer Engineering, University of Central Florida, Orlando, FL
Emails: eucer@crimson.ua.edu, mkisacik@ua.edu, gurbuz@ece.msstate.edu, srahman6@crimson.ua.edu, murat.yuksel@ucf.edu

***Abstract*—This study proposes a novel method for learning the congestion level of the power distribution system which designates the loading of a distribution feeder. A machine learning approach is proposed here to find a relating function between substation feeder power and local voltage. This model is, then, used to estimate real-time substation feeder power consumption using current local voltage measurements. This fully decentralized estimation of substation power consumption could facilitate more electric vehicle integration into the distribution grid without the need for real-time centralized control by a system aggregator. The concept is tested with real power loading data of a feeder located in the state of Alabama. The local voltage measurement data of a typical house residing in the downstream of the network of the same feeder is used to develop the learning algorithm.**

***Index Terms*—Machine Learning, Power Distribution System, Electric Vehicles, Congestion**

## I. Introduction

Transportation sector is one of the major sources of green house gas emissions. To reduce negative environmental consequences of conventional vehicles, transportation electrification has been considered as a promising solution [1]. Therefore, electrical vehicle (EV) technology has gained high popularity over the recent years, especially with the introduction of long range EVs. High penetration of electric vehicles (EVs) with uncontrolled charging is likely to cause transformer and/or line congestion in the power distribution grid. Among some adverse effects of this congestion are severe voltage drops, increased peak loading, thermal overheating, and even failure of equipment [2]–[7]. Congestion in the power distribution system is a situation where peak electricity demand nears the system capacity. Such a condition may violate thermal limits of critical power system components such as feeders and transformers. Grid congestion decreases operating efficiency and affects reliability of the power system. If, for instance, power lines are congested and operating at or near their thermal limits due to high demand, they will result in significant line losses [8].

Distribution system operators (DSOs) on the power grid have to manage congestion on a regular basis [9], [10]. Doing this congestion management with low overhead and in a scalable manner for many endpoints with dynamic load patterns (e.g., EVs) is a highly needed capability. To this end, this paper first performs a mathematical analysis of the distribution system to model the relation between an end-node voltage and total feeder power. In addition, correlation studies on simulated and experimental data are carried out to validate this relation. Our analysis shows that there is a quasi-linear relation between these variables. There have been similar efforts presented in the literature to demonstrate this relationship and propose some control solutions. [11] and [12] reveal the strong correlation between grid voltage and demand power, and propose a plug-and-play controller for household loads in accordance with the grid power demand. [13] demonstrates the voltage-demand relationship in a low-voltage (LV) distribution grid and discusses how this relationship can be leveraged for distributed load management. The voltage-demand relationship is further exploited and extended to EV charging control as decentralized solutions with local measurements [14], [15]. Voltage droop control is also often appealed as a decentralized solution in the distribution grid, particularly for photo-voltaic (PV) integration. [16] applies this idea to EV charging control with different droop models. [17] conclude that local control methods allow for a larger EV penetration but are not as capable at maintaining network parameters within their limits. Authors previously investigated impact of EV integration on historical end-node voltage [18] and implemented decentralized controllers that take action based on end-node voltages [19], [20].

Unlike the prior works, this study first utilizes the least squares estimation method as a machine learning tool. Based on learning performed on real data, we model this relationship as a linear function using Linear Regression (LR). Later, to improve the prediction accuracy and generalize the mapping in case of non-linearity, noise or variation, we build the model using Gaussian Process Regression (GPR). We further implement a Long-Short Term Memory (LSTM) network to support the prediction and compensate for the errors of GPR. These models are learned from substation power data and local voltage measurements. The innovative aspect of the proposed method is to estimate real-time substation total power consumption in a fully decentralized way. This decentralization reduces the need for the end-users to communicate with the substation (or centralized server) and enables integration of high-load end-users such as EVs to the grid in a plug-and-play manner. This framework will further help end-users to

This material is based upon work supported by the National Science Foundation under Award No 1755996.

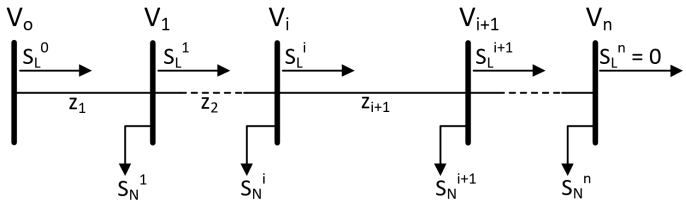


Figure 1: One-line diagram of a main radial distribution feeder.

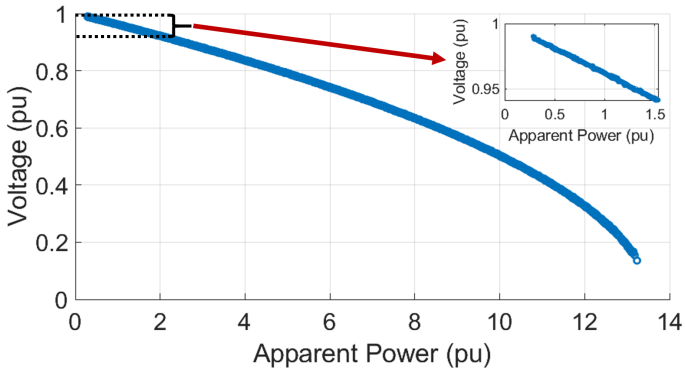


Figure 2: Mathematical relationship between end-node voltage vs. total feeder power ($S_L^0$) for a hypothetical loading case.

efficiently manage their electrical loads locally while maintaining a globally stable grid operation.

The main contributions of our work are as follows:

- Analysis and demonstration of the relationship between end-node voltage and total feeder power based on simulation results and empirical data collected from a real distribution grid.
- Machine learning (ML) based estimators (LR, GPR, and LSTM) to predict the total feeder power via local end-node voltage measurements.

The rest of the paper is organized as follows: Section II provides an analysis for the distribution system operation. Section III explains ML methodologies used in the study. Section IV describes data recording and processing technique. Section V shows the implementation of ML methods and provides results and discussion. Section V provides the concluding remarks and planned future study.

## II. Analysis of the Distribution System

A power distribution feeder leave a substation carrying three-phase power and reduce into single-phase through a single-phase center-tapped transformer. This transformer powers a group of houses and connects into a household through a single-phase line.

A typical single-feeder radial distribution grid model can be illustrated as in Fig. 1, where $S_L^i = P_L^i + jQ_L^i$ denotes the complex power flowing from node $i$ to node $i+1$ over a line impedance of $z_i = r_i + jx_i$. $S_N^i = P_N^i + jQ_N^i$ is the complex power drawn from node $i$, whereas the voltage of $i^{th}$ node is denoted by $V_i$. Then, the distribution model in Fig. 1 can be recursively solved for any node voltage $V_i$ by using the following **DistFlow** equations:

$$
\begin{aligned}
P_L^{i+1} &= P_L^i - r_{i+1}\frac{{P_L^i}^2+{Q_L^i}^2}{V_i^2} - P_N^{i+1} \\
Q_L^{i+1} &= Q_L^i - x_{i+1}\frac{{P_L^i}^2+{Q_L^i}^2}{V_i^2} - Q_N^{i+1} \\
V_{i+1}^2 &= V_i^2 - 2(r_{i+1}P_L^i + x_{i+1}Q_L^i) + (r_{i+1}^2 + x_{i+1}^2)\frac{{P_L^i}^2+{Q_L^i}^2}{V_i^2}
\end{aligned}
\tag{1}
$$

where $i = 0, 1, 2, \ldots, n$ [21]. The physics governed by DistFlow equations approximates to a linear relationship between any end-node voltage ($V_i = V_{end}$) and total substation loading ($S_L^0 = S_{total}$) over a small operating voltage range around its nominal such that $V_i = V_{rated} \pm \epsilon$ where $V_{rated}$ is the rated service voltage, i.e., 240 V. DistFlow equation (1) is a non-linear equation and can be linearized by neglecting the loss term $({P_L^i}^2 + {Q_L^i}^2) \cdot V_i^{-2}$. This simplification is based on a valid assumption and commonly known as **LinDistFlow** in the literature [21]. It significantly reduces the computation time to solve a distribution system model enjoying this linearity, and hence allows the development of faster algorithms. Fig. 2 shows this relationship between an end-node voltage ($V_{end}$) and total feeder power ($S_{total}$) in a custom radial distribution grid. As seen, the relationship remains fairly linear over the operating voltage range. This suggests that a linear function can be built to map these variables using the linear least squares estimation. This will be performed in the first part of this study. However, power grid specific dynamics (e.g., on-load tap changers (LTC) and voltage regulators (VR), cap banks, reactive power injections, node loading variations, and feeder voltage variations) might introduce noisy non-linear characteristics or curve shifts as illustrated in Fig. 3. These plots were obtained in a custom-sized distribution grid by varying the system parameters, i.e., by increasing load variations, substation voltage variation ($V_0$), reactive power generation, and power factor. In order to capture these variations and develop more generalized models for the relationship between $V_{end}$ and $S_{total}$, we will also use more advanced machine learning regression methods such as GPR and LSTM. This will be performed in the second part of this study.

## III. Methodology

In the proposed framework, the end-nodes will make loading decisions by inferring the distribution grid's congestion level from the local voltage $V_{end}$ they observe. In order to verify that the local voltage measurements can capture the distribution grid's congestion level, a correlation study is required to look for relations (correlations) between two random variables: (1) $S_{total}$ and (2) $V_{end}$. Correlation coefficient of $S_{total}$ and $V_{end}$ is a measure of their linear dependence. This dependency and high correlation allow us to construct a mapping from one variable to the other. If each variable has $N$ scalar observations, then the Pearson correlation coefficient is defined as:

$$
R(S_{total}, V_{end}) = \frac{1}{N-1}\sum_{i=1}^{N}\left(\frac{S_{total,i}-\mu_S}{\sigma_S}\right)\left(\frac{V_{end,i}-\mu_V}{\sigma_V}\right) \tag{2}
$$

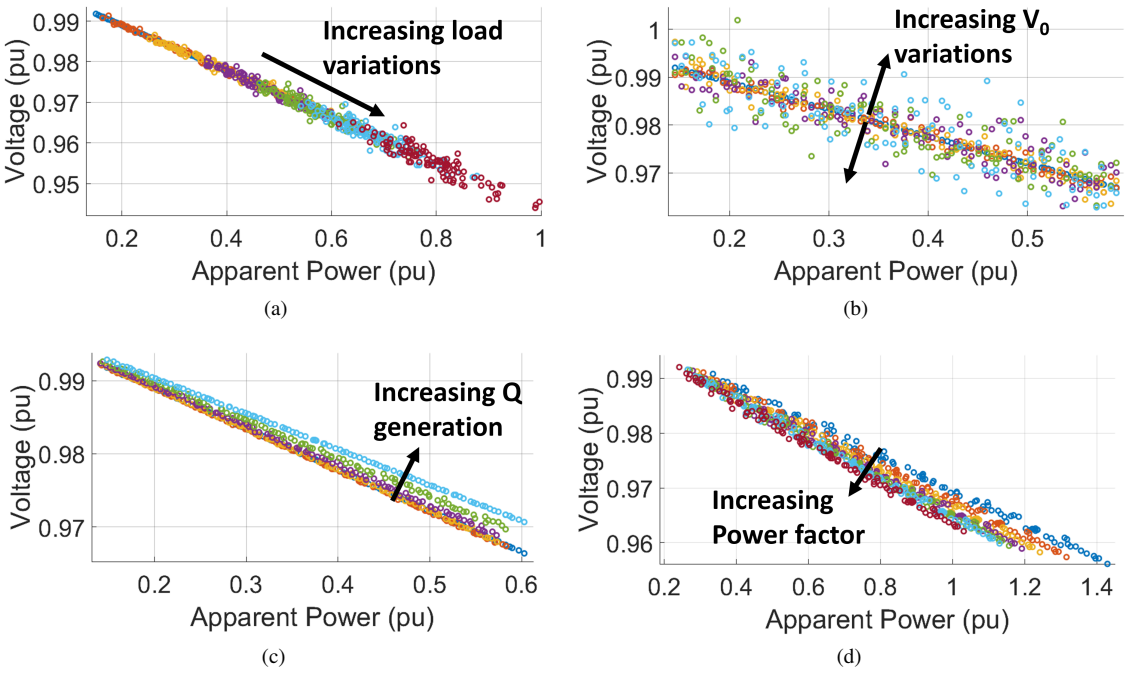


Figure 3: End-node voltage vs. feeder power relationships for different system parameters.

where $\mu_S$ and $\sigma_S$ are the mean and standard deviation of $S_{total}$, respectively; and $\mu_V$ and $\sigma_V$ are the mean and standard deviation of $V_{end}$, respectively.

To smooth fast variations of local voltage measurement, Exponential Weight Moving Average (EWMA) is applied on $V_{end}$ samples before the correlation against $S_{total}$ is calculated. For time period $t$, the voltage value smoothed by EWMA $\overline{V}_{end}(t)$ is determined as follows:

$$\overline{V}_{end}(t) = \alpha V_{end}(t) + (1-\alpha)\overline{V}_{end}(t-1) \tag{3}$$

where $\alpha$ is a parameter, which shows the rate at which the current observation will influence the calculated end-node voltage. Value of $\alpha$ is selected between 0 and 1; and $\alpha$ nearing to 0 means more weight is given to the older voltage data. In this study, $\alpha$ value is chosen to obtain the highest correlation coefficient between $S_{total}$ and $\overline{V}_{end}$.

As for the training and testing process, we measured 300 days of substation total feeder power ($S_{total}$) and end-node voltage ($\overline{V}_{end}$) data. For this study, we chose different subsets from the dataset that have 28 days of measurements. Out of these 28 successive days, the first 27 of them are used for training and the last day is used for testing. First, a least squares linear regression line is learned from the feeder and local voltage measurements to estimate the total feeder apparent power by the following model:

$$V_{end} = \theta_1 S_{total} + \theta_2, \tag{4}$$

where $\theta_1$ and $\theta_2$ are the slope and intercept parameters of the line, respectively. The least squares cost that is minimized to find the linear line parameters of (4) is given by:

$$\min_{m,c} \sum_{i=1}^{N} (\overline{V}_{end,i} - (\theta_1 S_{total,i} + \theta_2))^2. \tag{5}$$

The closed form solutions of the learning parameters ($\theta_1$ and $\theta_2$) are given accordingly as follows:

$$\theta_1 = \frac{\sum_{i=1}^{N}(S_{total,i} - \mu_S)(V_{end,i} - \mu_V)}{\sum_{i=1}^{N}(S_{total,i} - \mu_S)^2} \tag{6}$$

$$\theta_2 = \mu_V - \theta_1 \mu_S \tag{7}$$

In order to construct a mapping function from $\overline{V}_{end}$ to $S_{total}$ that can address the previously stated variations and improve the prediction accuracy, *Gaussian Process Regression (GPR)* learner is used in the second part. This learner has resulted in the minimum training error among other candidates including the linear least squares regression. Gaussian processes (GPs) allow non-parametric learning of a mapping function from noisy data by fitting Gaussian distributions conditioned on the data [22]. Due to the stated variations in the $S_{total}$ vs. $\overline{V}_{end}$ relationship and to model the time-dependent model correlations, we implemented a long-short term memory (LSTM) network [23] to further improve the prediction results. LSTM makes forecasts about the feeder loading based on historical data, and we can later use the forecast to check against the GPR estimates or even to compensate for it.

Finally, the trained model is tested for the real-time estimation of $S_{total}$ using real-time measurement of $\overline{V}_{end}$. Then, the root mean square error (RMSE) and mean absolute percentage error (MAPE) are calculated using (8) to check the accuracy of predictions made with the developed model.

$$\begin{aligned} RMSE &= \sqrt{\frac{\sum_{i=1}^{N}(S_{Estimated,i} - S_{Actual,i})^2}{N}} \\ MAPE &= \frac{1}{N}\sum_{i=1}^{N} \left| \frac{S_{Actual,i} - S_{Estimated,i}}{S_{Actual,i}} \right| \end{aligned} \tag{8}$$

## IV. System Description and Experimental Data

### A. System Description

In this study, a residential feeder located in Alabama is used to analyze the distribution system congestion. This feeder is serving approximately 2,000 customers through a radial line. There are four capacitor banks on the feeder rated at 1,200 kVAR, 900 kVAR, and two 600 kVARs. One of the 600 kVAR capacitors is located at the downstream of the house we are monitoring. There is also a 10% voltage regulator in the feeder connected at the upstream of the house in consideration. The transformer of the feeder is a load-tap changer. The feeder total apparent power data ($S_{total}$) is measured at every 15-minute interval. An eGauge smart meter [24] is installed to the house located at the downstream of the feeder, which measures one second resolution voltage ($V_{end}$) at the house end. The smart meter records data, and sends it to the cloud using local Wi-Fi connection. The end-node voltage data is publicly available at the University of Alabama institutional repository [25]. The data is collected in 2019 and 2020 for about a year. The substation data that powers the household is provided by Alabama Power which is operated by Southern Company.

### B. Dataset Generation and Pre-processing

Feeder apparent power data ($S_{total}$) is recorded at 15-minute intervals, whereas the local voltage ($V_{end}$) is measured at one-second resolution. Therefore, 15×24=96 samples of $S_{total}$ data and 60×60×24=86,400 samples of $V_{end}$ data are available per day. To equalize the number of samples, a down-sampling operation is applied on $V_{end}$ data.

The average of 60×15=900 samples is discretely calculated for each 15-minute interval in the $V_{end}$ data. The data processing is depicted on Fig. 4a. EWMA is applied on the down-sampled $V_{end}$ data to remove local dynamic and fast fluctuations (Fig. 4b). EWMA does not affect the sample size, but performs a filtering action on $V_{end}$ data. For different $\alpha$ values ranging from 0.01 to 1.0 with 0.01 increments, $\overline{V}_{end}(t)$ is calculated according to (3). Then, the correlation coefficient between $S_{total}$ and $\overline{V}_{end}$ is computed for each $\alpha$ value. The optimum $\alpha$ value is calculated as 0.07 where the maximum correlation co-efficient is observed.

## V. Machine Learning Models

To understand how closely $S_{total}$ and $\overline{V}_{end}$ data in a scatter plot fall along a straight line, a correlation study is performed. Correlation coefficient ($R$) measures the strength and direction of a linear relationship. The absolute value of $R$ close to one means the data are described better by a linear equation. Data sets with values of $R$ close to zero show little to no straight-line relationship. $R$ for five weekdays of July 2019 is found as follows: July $15^{th} = -0.8227$, July $16^{th} = -0.9870$, July $17^{th} = -0.9479$, July $18^{th} = -0.9765$, and July $19^{th} = -0.9842$. In all cases, the absolute values of $R$ are greater than 0.8. It clearly indicates that $S_{total}$ and $\overline{V}_{end}$ data are aligned and well correlated on a straight line in the scatter plot.

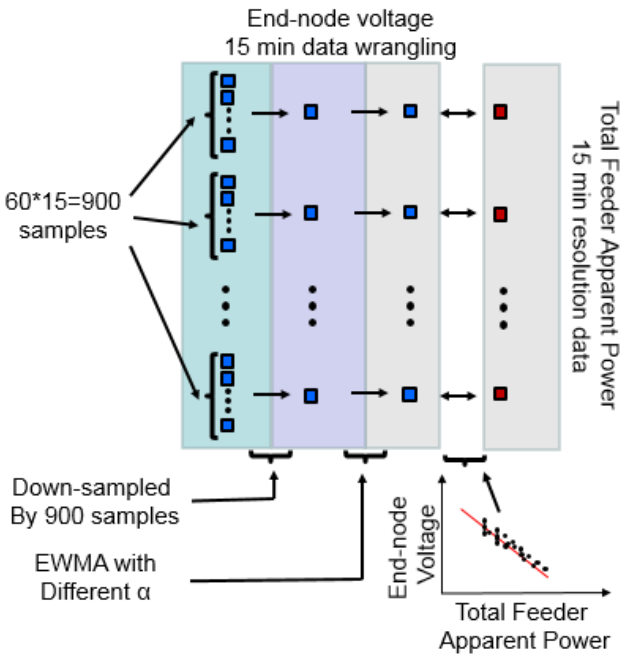


(a)

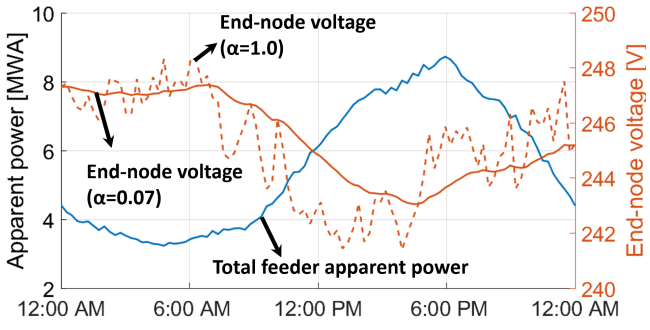


(b)

Figure 4: (a) Data wrangling for power and voltage data and (b) EWMA applied on local $V_{end}$ and substation power.

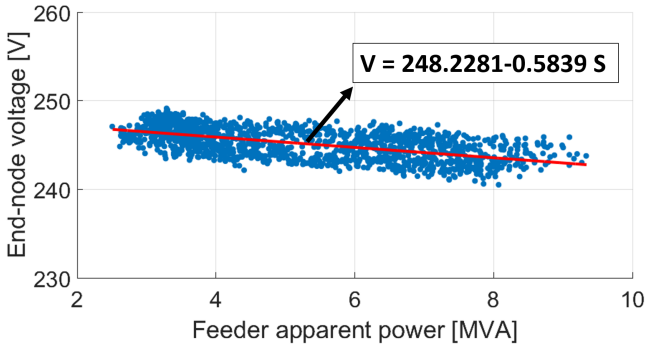


Figure 5: Linear relationship between end node voltage and total feeder power for 16 days of July 2019.

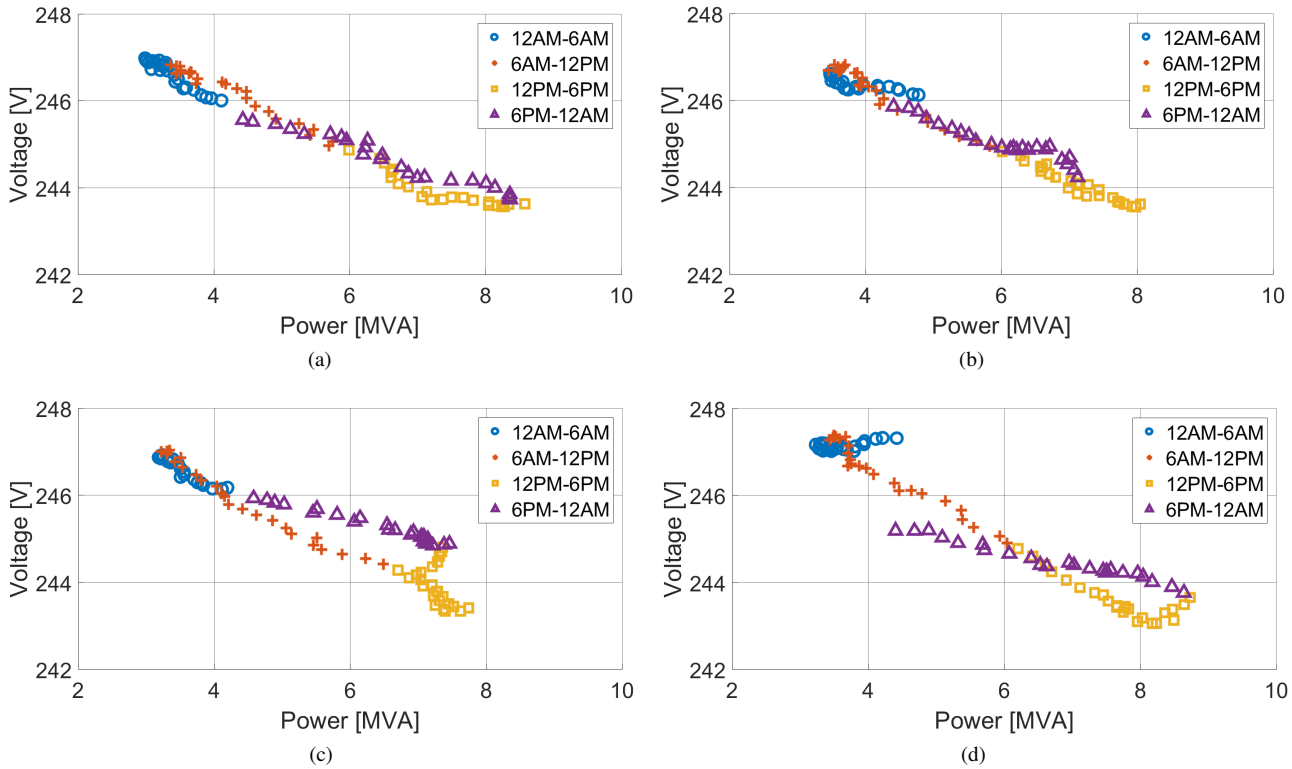


Figure 6: End-node voltage vs. feeder power for four days: (a) July-16, (b) July-19, (c) July-28, and (d) July-29 with each day split into four time intervals (colored).

To see the relationship between $S_{total}$ and $V_{end}$, an $X/Y$ (scatter) plot is used with $S_{total}$ along the horizontal axis and $V_{end}$ on the vertical axis. Fig. 5 is constructed with $S_{total}$ and pre-processed $V_{end}$ data collected from the feeder and the eGauge meter respectively. The experimental data also indicates the quasi-linear relation shown mathematically in Section II. Hence, we model the relationship between $S_{total}$ and $V_{end}$ linearly, i.e., $V_{end} = \theta_1 \cdot S_{total} + \theta_2$ where $(\theta_1, \theta_2)$ are model parameters to be learned. To define their relationship, a line equation is constructed. For instance, the parameters of the linear line fit to the data collected over a total of 16 days of July 2019 are estimated as $\theta_1 = -0.5839$ and $\theta_2 = 248.2281$ (Fig. 5).

The insights from analyses and empirical results suggest using a linear model using LR. We will first investigate the performance of this model and present the results of LR. However, as previously stated, this linear relationship might be exposed to noise, shift, or some other disturbances due to various dynamics taking place in the grid. Different times of the day might also have different regulations and thus exhibit different trends. To illustrate this, four July 2019 days (July 16-19-28-29) were split into four time intervals (12AM-6AM, 6AM-12PM, 12PM-6PM, 6PM-12AM), and their end-node voltages are plotted against the corresponding day's total feeder power and shown in Fig. 6. We can clearly see that the parameters of the linear relationship are fairly constant on some days (Fig. 6a and Fig. 6b) whereas they are slightly changed on other days (Fig. 6c and Fig. 6d) especially during 6PM-12AM (purple). It can also be seen that different time frames in a single day have different quasi-linear relations. To that end, GPR and LSTM models will be tested against classical LR to improve the prediction performance and the results will be compared.

To demonstrate how accurately the proposed models can predict the total feeder power consumption using local end-node voltage measurements, we put them to a test using four different days (i.e. Aug. 10 2019, Sept. 8 2019, Jan. 7 2020, and Apr. 17 2020). We trained the ML models using MATLAB's *Regression Learner Toolbox*. This toolbox has optimized hyper-parameters settings to automate the selection of hyper-parameter values. To protect against overfitting, we used cross-validation by partitioning the dataset into five folds. For time series forecasting, we used an LSTM layer with 200 hidden units and trained the model using MATLAB's *trainNetwork* function.

An important observation is that due to variations in system model parameters (as explained in Fig. 3) for different days and for different time frames within a day, the system modelling should understand such changes for better estimation accuracy. As an effort towards addressing this, we included *the day of the week and time of the day information*, which are introduced as two new input features into the learning algorithm. After these updates, the dataset has three inputs (voltage, time interval, and day of week) and one output (feeder power) for each data sample.

Fig. 7 shows the three estimates, i.e., LR, GPR, and LSTM, for the actual total feeder power. The corresponding end-node voltage is also provided on the same plots. The corresponding estimation errors are calculated in terms of RMSE and MAPE

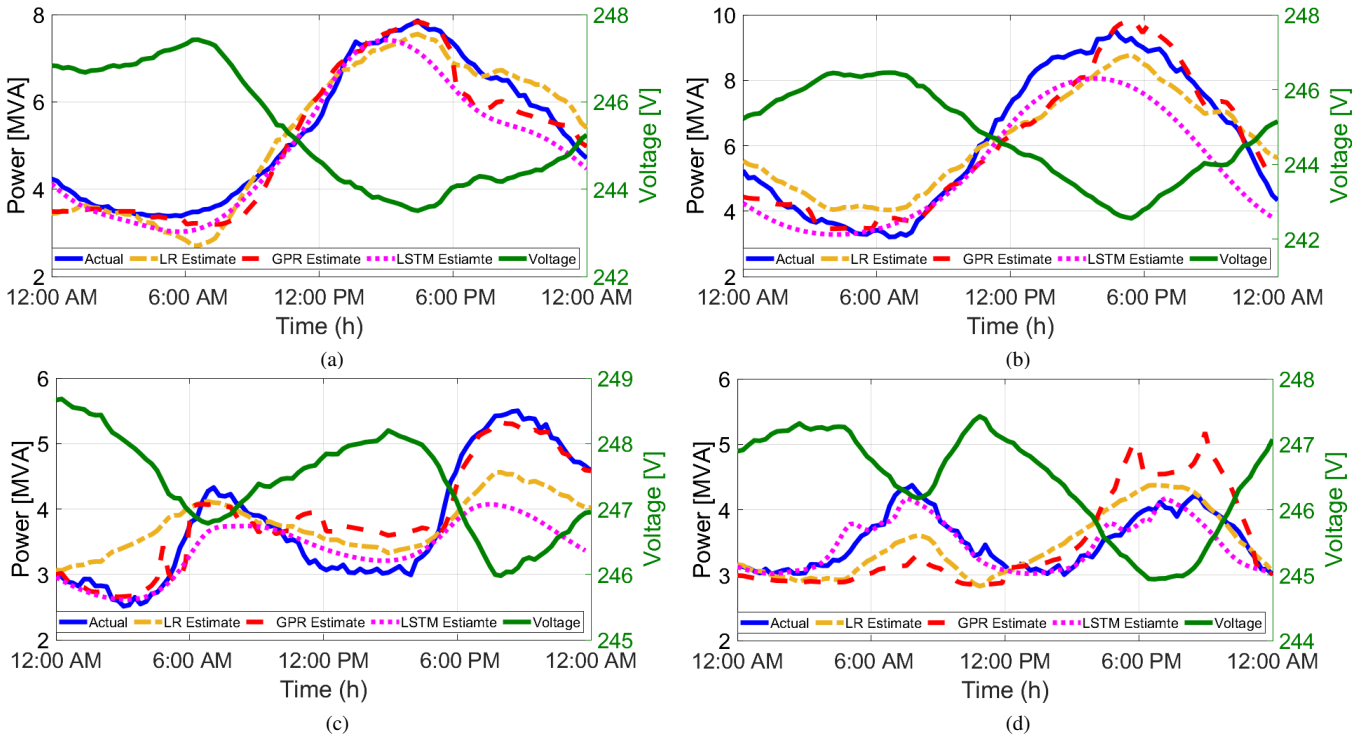


Figure 7: Actual and estimated total feeder power consumption using LR, GPR and LSTM, and end-node voltage for (a) Aug. $10^{th}$ of 2019, (b) Sept. $8^{th}$ of 2019, (c) Jan. $7^{th}$ of 2020, and (d) April $17^{th}$ of 2020.

(i.e. (8)) and provided in Table I (best results are shown in bold). The correlation coefficients between the actual power vs. end-node voltage (Corr(S, V)) and the actual power vs. the estimated values (Corr(S, LR), Corr(S, GPR), Corr(S, LSTM)) are also computed and presented in Table II (best results are shown in bold). The explanation on Fig. 7 and Tables I and II are provided below.

Fig. 7 first shows that LR predictions are able to follow the trends in the total feeder power just by monitoring the local voltage as suggested earlier in the paper. Therefore, the performance of LR is acceptable to some extent but there is room for development for better prediction accuracy via utilizing GPR and LSTM. For instance, Table I uncovers that LR estimate errors are higher than that of GPR (except for April $17^{th}$). Although regression can be quite successful in constructing a mapping function to predict the total power using end-node voltage and other features (time interval and day of week), it is still prone to errors, i.e., the learned relationship becomes highly invalid/violated for the day of prediction. We see such a problem with the GPR estimate especially on $17^{th}$ of April. To deal with this problem, we also implemented an LSTM network to make a prediction on the next day's total power by providing the previous days' data. This can serve as a guidance for the final prediction and help us check the accuracy of GPR.

Both estimations (GPR and LSTM) for Aug. $10^{th}$ (Fig. 7a) and Sept. $8^{th}$ (Fig. 7b) closely follow the actual value though they are slightly off especially after 5PM. Table I shows that GPR made better estimates compared to LSTM, suggesting that the final prediction should be closer to that of GPR for these two days. Fig. 7c and Fig. 7d demonstrate the results for Jan. $7^{th}$ and Apr. $17^{th}$. We see double peaks in the total power consumption since the data belongs to different seasons of the year. On Jan. $7^{th}$, the LSTM estimate stays below the actual consumption, however, this can be compensated by the GPR estimate since its error values are much smaller (Table I). Interestingly, the LSTM estimate between 12PM-6PM is more accurate than that of the GPR estimate. This suggests that the final estimate could be weighted more towards LSTM during this time interval. On Apr. $17^{th}$, we see the GPR estimate is far off the actual consumption even though it can still detect the trends (peaks) in the consumption via voltage mapping. This is because the GPR estimation is based on the measured local voltage and the voltage of this day is poorly correlated with the actual power resulting in a correlation coefficient of -0.6745 (Table II). However, the LSTM estimate gives a much

Table I: RMSE and MAPE scores for LR, GPR, LSTM estimations.

| Days | RMSE (LR) | RMSE (GPR) | RMSE (LSTM) | MAPE (LR) | MAPE (GPR) | MAPE (LSTM) |
|---|---|---|---|---|---|---|
| Aug. 10, 2019 | 0.4154 | **0.3866** | 0.4916 | 0.0613 | **0.0575** | 0.0716 |
| Sept. 8, 2019 | 0.7573 | **0.5954** | 1.0040 | 0.1051 | **0.0740** | 0.1271 |
| Jan. 7, 2020 | 0.5731 | **0.3420** | 0.7023 | 0.0840 | **0.0771** | 0.1075 |
| Apr. 17, 2020 | 0.3703 | 0.5758 | **0.1826** | 0.0812 | 0.1277 | **0.0366** |

Table II: Correlation scores between actual power vs. actual voltage, LR, GPR, and LSTM estimations.

| Days | Corr (S, V) | Corr(S, LR) | Corr(S, GPR) | Corr(S, LSTM) |
|---|---|---|---|---|
| Aug. 10, 2019 | -0.9690 | 0.9690 | 0.9761 | **0.9762** |
| Sept. 8, 2019 | -0.9770 | **0.9770** | 0.9622 | 0.9691 |
| Jan. 7, 2020 | -0.9174 | 0.9174 | **0.9368** | 0.8587 |
| Apr. 17, 2020 | -0.6745 | 0.6269 | 0.5807 | **0.9074** |

more accurate prediction resulting in the lowest RMSE value among all testing results. For this day, the compensation for the final prediction should be weighted more towards the LSTM estimate.

## VI. Conclusions and Future Work

This study investigates how loading of grid assets, such as substation transformers and feeders, can be mapped to local voltage, and how this mapping can be used to locally estimate the network congestion level in real time. Correlation study revealed that the relationship between the feeder power and the local voltage is highly linear, and thus can be formulated by a linear function using LR. It has been showed that the degree of correlation can be increased with EWMA by filtering out the noises present in the local voltage data. To validate the approach, the study estimated the real-time feeder power of a real substation in Alabama by using the real-time end-node voltage, day, and time information using RL, GPR, and LSTM. The results showed that the estimations closely follow the actual value for the testing days (the best RMSEs ranging from 0.1826 to 0.5954). However, we also observed that the estimates seem off from the actual power consumption for some days. This suggests the presence of other voltage regulation actions taking place at the upstream/downstream network that can cause violation in the derived mapping function and result in low accuracy. In those cases, the best estimate can be obtained using a weighted combination of estimates (such as GPR and LSTM) since one may perform better than the other for a particular day compensating the error. Therefore, our future study will involve how to combine the results of both estimates to make more accurate unified predictions of critical feeder operation points for the purpose of enhancing and improving the grid operation.

## Acknowledgement

The authors would like to thank Brooke Williams, Tom Canada, Derl Rhoades, and Andrew Ingram from Southern Company for their help and support in accessing the substation feeder data, and for thoughtful discussions.

## References

[1] (2015) Study: Electric vehicles can dramatically reduce carbon pollution from transportation, and improve air quality. https://www.nrdc.org/experts/luke-tonachel/study-electric-vehicles-can-dramatically-reduce-carbon-pollution. [Online; accessed 10-Jan-2020].

[2] F. Erden, M. C. Kisacikoglu, and O. H. Gurec, "Examination of EV-grid integration using real driving and transformer loading data," in *Int. Conf. Elect. Electron. Eng.*, 2015, pp. 364–368.

[3] L. P. Fernandez, T. G. S. Roman, R. Cossent, C. M. Domingo, and P. Frias, "Assessment of the impact of plug-in electric vehicles on distribution networks," *IEEE Trans. Power Syst.*, vol. 26, no. 1, pp. 206–213, Feb. 2011.

[4] S. Shafiee, M. Fotuhi-Firuzabad, and M. Rastegar, "Investigating the impacts of plug-in hybrid electric vehicles on power distribution systems," *IEEE Trans. Smart Grid*, vol. 4, no. 3, pp. 1351–1360, 2013.

[5] E. Veldman and R. A. Verzijlbergh, "Distribution grid impacts of smart electric vehicle charging from different perspectives," *IEEE Trans. Smart Grid*, vol. 6, no. 1, pp. 333–342, 2015.

[6] N. Leemput, F. Geth, J. Van Roy, A. Delnooz, J. Buscher, and J. Driesen, "Impact of electric vehicle on-board single-phase charging strategies on a flemish residential grid," *IEEE Trans. Smart Grid*, vol. 5, no. 4, pp. 1815–1822, 2014.

[7] K. Clement-Nyns, E. Haesen, and J. Driesen, "The impact of charging plug-in hybrid electric vehicles on a residential distribution grid," *IEEE Trans. Power Syst.*, vol. 25, no. 1, pp. 371–380, Feb. 2010.

[8] S. Huang, Q. Wu, L. Cheng, and Z. Liu, "Optimal reconfiguration-based dynamic tariff for congestion management and line loss reduction in distribution networks," *IEEE Trans. Smart Grid*, vol. 7, no. 3, pp. 1295–1303, May 2016.

[9] O. Sundstrom and C. Binding, "Flexible charging optimization for electric vehicles considering distribution grid constraints," *IEEE Trans. Smart Grid*, vol. 3, no. 1, pp. 26–37, Mar. 2012.

[10] J. Hu, S. You, M. Lind, and J. Østergaard, "Coordinated charging of electric vehicles for congestion prevention in the distribution grid," *IEEE Trans. Smart Grid*, vol. 5, no. 2, pp. 703–711, Mar. 2014.

[11] T. Ganu, J. Hazra, D. P. Seetharam, S. A. Husain, V. Arya, L. C. De Silva, R. Kunnath, and S. Kalyanaraman, "nplug: A smart plug for alleviating peak loads," in *Int. Conf. on Future Syst.*, May. 2012.

[12] T. Ganu, D. P. Seetharam, V. Arya, J. Hazra, D. Sinha, R. Kunnath, L. C. D. Silva, S. A. Husain, and S. Kalyanaraman, "nplug: An autonomous peak load controller," *IEEE J. Sel. Areas Commun.*, vol. 31, no. 7, pp. 1205–1218, July 2013.

[13] L. Xia, T. Alpcan, I. Mareels, M. Brazil, J. de Hoog, and D. A. Thomas, "Modeling voltage-demand relationship on power distribution grid for distributed demand management," in *Australian Control Conf. (AUCC)*, Nov. 2015.

[14] L. Xia, T. Alpcan, I. Mareels, M.Brazil, J. de Hoog, and D. A. Thomas, "Local measurements and virtual pricing signals for residential demand side management," *Sustain. Energy, Grids and Netw.*, Dec. 2015.

[15] L. Xia, J. de Hoog, T. Alpcan, M. Brazil, I. Mareels, and D. Thomas, "Electric vehicle charging: A noncooperative game using local measurements," *IFAC Proc. Volumes*, vol. 47, no. 3, pp. 5426–5431, 2014.

[16] F. Geth, N. Leemput, J. Van Roy, J. Büscher, R. Ponnette, and J. Driesen, "Voltage droop charging of electric vehicles in a residential distribution feeder," in *IEEE PES ISGT Europe*, Oct. 2012, pp. 1–8.

[17] P. Richardson, D. Flynn, and A. Keane, "Optimal charging of electric vehicles in low-voltage distribution systems," in *IEEE Power Energy Soc. General Meeting*, July 2012.

[18] E. Ucer, M. C. Kisacikoglu, and A. C. Gurbuz, "Learning EV integration impact on a low voltage distribution grid," in *IEEE Power Energy Soc. General Meeting*, Aug. 2018, pp. 1–5.

[19] E. Ucer, M. C. Kisacikoglu, M. Yuksel, and A. C. Gurbuz, "An internet-inspired proportional fair EV charging control method," *IEEE Syst. J.*, vol. 13, no. 4, pp. 4292–4302, Dec. 2019.

[20] E. Ucer, M. C. Kisacikoglu, and M.Yuksel, "Analysis of decentralized AIMD-based EV charging control," in *IEEE Power Energy Soc. General Meeting*, Aug 2019, pp. 1–5.

[21] M. Baran and F. F. Wu, "Optimal sizing of capacitors placed on a radial distribution system," *IEEE Trans. Power Del.*, vol. 4, no. 1, pp. 735–743, 1989.

[22] M. F. Huber, "Recursive gaussian process regression," in *IEEE Int. Conf. Acoustics, Speech Signal Process.*, 2013, pp. 3362–3366.

[23] S. Hochreiter and J. Schmidhuber, "Long short-term memory," *Neural Comput.*, vol. 9, no. 8, p. 1735–1780, Nov. 1997.

[24] Energy monitoring systems for residential and commercial applications. http://www.egauge.net/. [Online; accessed 31-Jan-2018].

[25] E. Ucer, S. Rahman, A. McDonald, and M. Kisacikoglu. (2019) Residential active/reactive power consumption, voltage, and frequency data for a house in Alabama. [Dataset] https://ir.ua.edu/handle/123456789/6346. [Online; accessed 15-Jul-2020].